Journal of BUON **17:** 526-532, 2012

ORIGINAL ARTICLE

Dosimetric consequences of pancreatic tumor motion when predetermined treatment margins are employed during intensity-modulated radiation therapy

J. Shen[1], J.M. Metz[1], T.C. Zhu[1], J. Panetta[1], J.C. Finlay[1], M. Xu-Welliver[1], J.P. Plastaras[1], V. Bar Ad[2], S. Both[1]

[1]Department of Radiation Oncology, University of Pennsylvania School of Medicine, Philadelphia; [2]Department of Radiation Oncology, Thomas Jefferson University Hospital, Pennsylvania, Philadelphia, USA

Summary

Purpose: *To quantify the dosimetric consequences of pancreatic tumor motion on the pancreatic intensity-modulated radiation therapy (IMRT) plans.*

Methods: *Dose map of IMRT plans for 5 patients with pancreatic cancer were measured using a 2D diode array placed on a computer-controlled platform to simulate 2D pancreatic tumor motion. Dosimetric analysis was then performed to obtain IMRT quality assurance (QA) passing rates. The convolution method, which used a motion kernel to simulate 2D pancreatic motion, was also applied to the treatment and phantom verification plans for a wide range of magnitudes of motion (0.8-2.0 cm). The resulting motion-convolved verification dose maps (VDMs) were compared with the dynamic measurements to evaluate IMRT QA passing rates as well as the dose-volume histogram, the $V_{95\%}$ of the planning target volume (PTV) and $V_{98\%}$ of the clinical target volume (CTV).*

Results: *While CTV coverage was maintained when the simulated pancreatic tumor drifted inside the PTV with magnitudes of 1.0 cm and 1.5 cm, the $V_{95\%}$ of the PTV was reduced by 10% and 17%, respectively. We also found that the differences between the measurements and the static VDMs increased proportional to the amplitude of motion, while the agreement between the measurements and the motion-convolved VDMs was excellent for any magnitude of motion.*

Conclusions: *When the 4D technique is not available, predetermined margins must be used carefully to avoid possible under-dose to the target. Additionally, the phantom results show that the kernel convolution method provides an accurate evaluation of the dosimetric impact due to tumor motion and it should be employed in the planning process.*

Key words: convolution, dosimetry, IMRT, pancreas, pancreatic cancer, tumor motion

Introduction

Recent studies have indicated that IMRT dose escalation to pancreatic tumors is achievable with acceptable normal tissue toxicity and superior dosimetry compared to that of 3D conformal RT [1-5]. However, pancreatic tumors show a significant, highly variable respiratory associated motion, which may adversely affect the dosimetric outcome of IMRT techniques [6]. Although studies in the past have used large, population-based margins to account for pancreatic tumor motion [1-5], individually assessing the motion may be essential to the accurate delivery of IMRT since target motion will affect dose distribution, especially for highly conformal IMRT treatments [7-11].

Pancreatic tumor motion has been examined and quantified using various methods [7-10]. Movement in the lateral direction is considered to be negligible (<2 mm), but motion in the craniocaudal (CC) and anteroposterior (AP) directions was found to be highly variable among patients up to 40 mm and 13 mm in the CC and AP directions, respectively [7-10]. If advanced imaging modalities such as 4D CT are not available to accurately evaluate the tumor motion, predetermined margins based on data from large populations must be employed as an approximation to account for the motion. Yet, due to the variation of the motion among patients, the use of predetermined margins is associated with the risk of under-dosing the tumor or over-dosing the organs at risk (OARs) [10]. In order to assess this risk, it is

Correspondence to: Jiajian Shen, PhD. Department of Radiation Oncology, University of Pennsylvania, School of Medicine, 3400 Spruce street, Philadelphia, PA 19 104, USA. Tel: +1 215 614 6086, Fax: +1 215 349 5978, E-mail: Jiajian.Shen@uphs.upenn.edu

Received 21-02-2012; Accepted 16-03-2012

necessary to quantify the correlation between the magnitude of motion and the dosimetric outcome.

The purpose of this study was to experimentally quantify the dosimetric effect of pancreatic tumor motion and to verify the results by a convolution method that used a motion kernel.

Methods

In the study, we placed a 2D diode array on a moving platform that simulated pancreatic tumor movement (see below). We then collected the doses delivered to the diode array by a linear accelerator both when the platform was stationary and when it was moving. A range of typical magnitudes of tumor motion was used to determine the effect of magnitude on the accuracy of radiation delivery.

IMRT plan data

Five patients with pancreatic cancer were selected for this study. For each patient, a radiation oncologist contoured the CTV, and then added a margin of 1.0 cm to the CTV to define the PTV [12,13]. Sliding-window IMRT plans (Varian 2300IX, Palo Alto, CA) were generated in the Eclipse (Varian Medical Systems, Palo Alto, CA) treatment planning system (TPS) using 5-7 coplanar beams. For each plan, 100% of the CTV and PTV were specified to receive 98% and 95% of the prescribed dose (50.4 Gy), respectively, and the dose constraints to the OARs were as follows: a maximum dose of 45 Gy to the spinal cord, constraints of 50% of the volume of the liver to <30 Gy, and 50% of the kidney volume <18 Gy. Phantom verification plans (PVPs) were generated from the treatment plans within the TPS, and 2D static VDMs in the coronal plane were exported to the 2D diode array data.

Motion measurements

2D diode arrays (Mapcheck, Sun Nuclear Corporation, Melbourne, FL) are well-established devices for IMRT treatment-plan QA and serve as an important check of the accurate delivery of plans [14-17]. In order to simulate tumor motion, the diode array was placed on a platform that was linked to a computer-controlled step motor (Velmex, Inc., East Bloomfield, NY). The three wheels of the platform moved along Styrofoam wedges, the angles of which were chosen to be 19° so that the ratio of the magnitudes of motion between the CC and AP directions modeled that for the tumor motion reported in the literature, ~3:1 [7-10]. The motor drove the platform along the wedges, achieving simultaneous motion in what would be the CC and AP directions for a supine patient. The period of the movement was 4 sec, to simulate respiratory motion (15 per min), while there were two amplitudes used in the CC direction, 1.0 cm and 1.5 cm. Here, 1.0 cm is the size of the representative predetermined margin used to ensure that the CTV received adequate dose, and 1.5 cm is the value used to represent a tumor that moves beyond the predetermined margin. Note that the magnitudes of motion given in this study are the radii of the motion (one half of the peak-to-peak amplitudes).

For each PVP, diode array data were acquired both with the diode array stationary and undergoing the periodic motions described above. Each set of measurements using the motion platform was started at a random phase and, in order to reduce the random error associated with this phase, each plan was delivered and measured three times. The resulting diode array dose maps were then averaged, producing dose maps that are herein termed the dynamic diode measurements, in contrast with the static diode measurements.

Data analysis

The measurements and the static VDMs were analyzed within the Mapcheck software. IMRT QA passing rates were obtained here by applying percentage difference and distance to agreement (DTA) criteria. In this passing rate analysis, the most stringent passing criteria (90% at 3%, 3 mm DTA, threshold (TH)=10%) were applied throughout the study, unless otherwise noted [18]. A typical dose map analysis is shown in Figure 1.

Motion convolution

The convolution method, the basic algorithm of which has been described previously [19-21], has been used to correct treatment plans for respiratory-induced change in dose, involving either dose or fluence convolution [19-21]. This method convolves the static dose/fluence distribution with a motion kernel to generate a motion-convolved dose/fluence distribution. The motion kernel is the probability distribution function that describes the nature of tar-

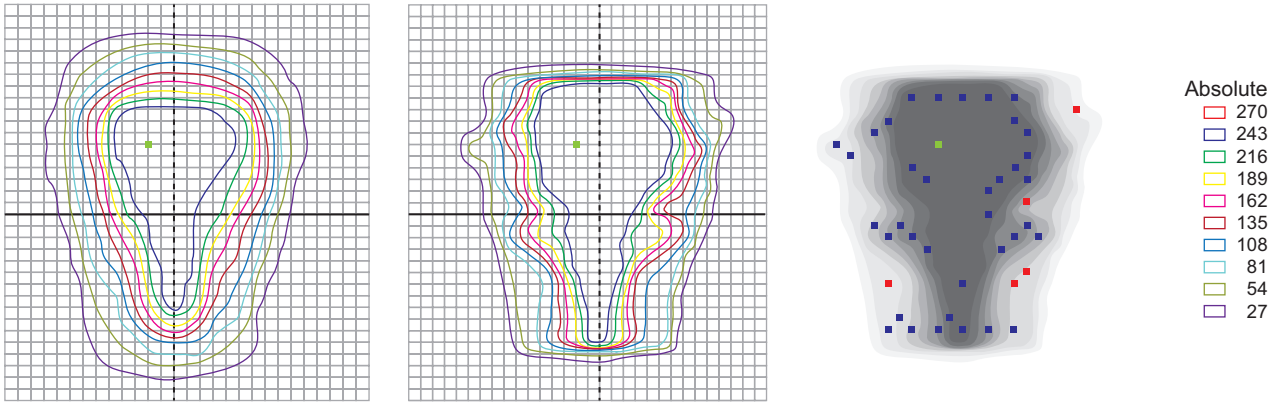

Figure 1. A typical dose map passing rate analysis. The left panel shows the measured dose map for a 2D magnitude of motion of 1.5 cm; the middle panel shows the static VDMs; the right panel shows the comparison of these two dose maps. Red (hot) and blue (cold) are points that failed the given passing criterion. 196 detectors were included in this analysis; the passing rate was only 77.6%. The green dot is the normalization point.

get motion, e.g. the probability that the pancreas will be a particular distance from the starting position.

The dose convolution algorithm used in this study is derived from the work of Lujan et al. in 1999 [19], but involves a 2D dose convolution instead of the 1D convolution described by Lujan et al. in 1999 [19]. Our simulations were designed to mirror the experimental setup described above, based upon a sinusoidal wave with a period of 4 sec. The selected magnitudes of motion in these convolution simulations ranged from 0.8 cm to 2.0 cm for the CC direction, spanning all of the reported amplitudes in that direction. Each magnitude of motion in the AP direction was one third of its respective magnitude in the CC direction, as modeled by the 19° wedge used in the experiment. Last, the lateral motion was not considered in the convolution because pancreatic tumors display negligible lateral movement.

We used the above method to perform a kernel convolution (MATLAB [22]), with the static diode measurements and the static volume dose calculated in the PVP, creating motion-convolved measurements and volume dose respectively. In order to compare with the 2D dynamic measurements, we extracted 2D slices from the motion-convolved volume dose; the slices were parallel to the 2D coronal dose plane and at the same depth as that of the static 2D verification plane. These extracted coronal dose maps are herein referred to as the motion-convolved VDMs, in contrast with the static VDMs. The dynamic measurements were compared with the motion-corrected VDMs, and the passing rates were obtained for all 5 patients. (A typical comparison of the above dose maps is given in Figure 2, with the agreement between these two dose maps shown to be almost ideal).

The motion-convolved VDMs were also manipulated to have the same data format as the measurements obtained with the diode array, converting them to dose maps that are referred to herein as simulated diode measurements. These simulated diode measurements resembled the real measurements as expected, since both included the effect of motion. They were then compared with the static VDMs to obtain the simulated IMRT QA passing rates.

Target coverage and OAR sparing

In order to investigate how pancreatic tumor motion affects the dose to the target and OARs, we exported the patient volume doses from TPS and applied our motion convolution method (MATLAB [22]) to those volume doses. The respiration-induced tumor motion is generally not symmetric, with the majority of time spent at the exhale position [19]. Therefore, the motion kernel was not derived from the symmetric sinusoidal wave but a fit function to the nature of the abdomen motion due to breathing [19]. For the motion-convolved plans, the dose-volume histogram (DVH) parameters of the CTV, PTV and OARs were analyzed. Two clinically important coverage parameters, $V_{95\%}$ (percent of volume receiving >95% of the prescription dose) of the PTV and $V_{98\%}$ (percent of volume receiving >98% of the prescription dose) of the CTV were obtained.

Results

A passing rate analysis was performed using various passing criteria, over the range of the magnitudes of motion used (margin of tumor motion for all plans was 1.0 cm). Specifically, the IMRT QA passing rates were calculated for the dynamic diode measurements relative to the static and motion-convolved VDMs and for the simulated measurements relative to the static VDMs. These passing rates were then averaged over all 5 patients.

Table 1 presents the passing rates for the dynamic diode measurements relative to the static VDMs, with their standard deviations. For the 1.5 cm magnitude of motion, all dose maps failed to pass any acceptable criteria (90% at 3%, 5%, and 7%; 3 mm and 4 mm DTA; TH=10%). By contrast, all plans passed even the strict-

Table 1. The mean passing rates and standard deviations for different passing rate criteria

Magnitude of motion (cm)	*Passing criteria (Error %, DTA, TH)*	*Mean passing rate ± STD*
0 (static)	3% 3 mm 10%	98.8% ± 1.2%
1.0	3% 3 mm 10%	90.8% ± 4.1%
1.5	3% 3 mm 10%	74.9% ± 3.8%
	5% 3 mm 10%	78.4% ± 2.8%
	7% 4 mm 10%	86.2% ± 1.9%

DTA: distance to agreement, TH: threshold, STD: standard deviation

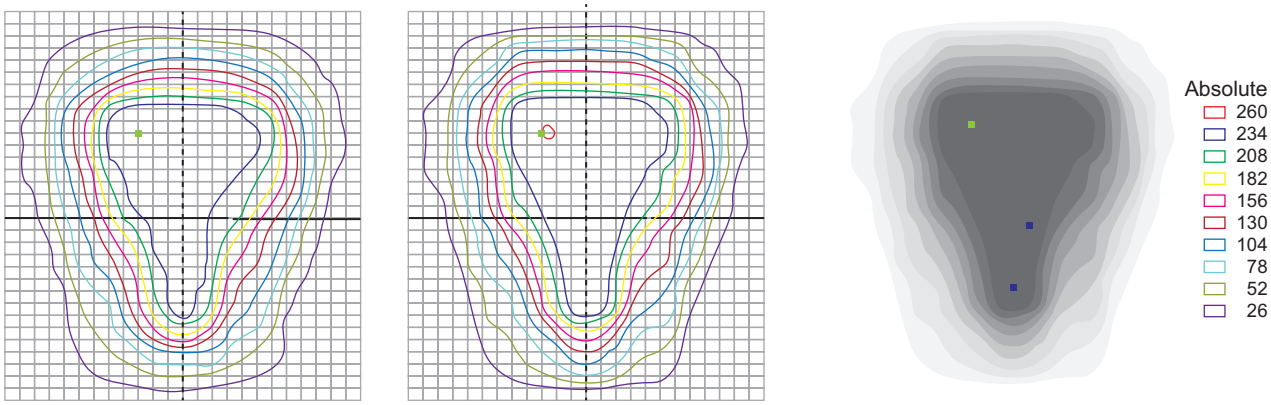

Figure 2. A typical dose map passing rate analysis. The left panel shows a diode measurement with a 2D magnitude of motion of 1.5 cm; the middle panel shows the motion-convolved VDMs; the right panel shows the comparison of these dose maps. 207 detectors were included in the analysis; the passing rate was 99%. The green dot is the normalization point.

est criteria (90% at 3%, 3 mm DTA, TH=10%) when the amplitude was reduced to 1.0 cm.

Figures 3 and 4 show the various passing rates, calculated using the strictest criteria, plotted across the range of magnitudes of motion employed. The passing rates for the dynamic diode measurements relative to the motion-convolved VDMs are each ≥98.5% (Figure 3), expectedly high since the motion-convolved verification plans modeled the actual delivery of the machine more accurately than the static verification plans did. Moreover, the high passing rates strongly indicate that when an IMRT plan is delivered, the motion kernel convolution accurately calculates the actual dose to a moving phantom target.

The passing rates for the simulated measurements relative to the static VDMs are linearly correlated to the magnitudes of motion and are always higher than the corresponding rates for the dynamic measurements relative to the static VDMs (Figure 4). Note that the passing rate of 90% for the simulated measurements corresponds to a magnitude of ~1.1 cm, indicating that tumor motion that extended beyond the 1.0 cm treatment margin significantly affected the delivery of dose.

Figure 5 shows the relationships of the magnitude of motion to the PTV and CTV coverage and IMRT QA passing rate. The $V_{95\%}$ of the PTV and the IMRT QA passing rate were reduced significantly as the magnitude of pancreatic tumor motion increased. When the magnitude was 1.0 cm, the $V_{95\%}$ of the PTV was reduced by 10% from its value for the stationary situation; when the largest tumor motion (2.0 cm) was applied, it was reduced by 26%. The IMRT QA passing rate was ~93% when the amplitude of 1.0 cm was applied, and

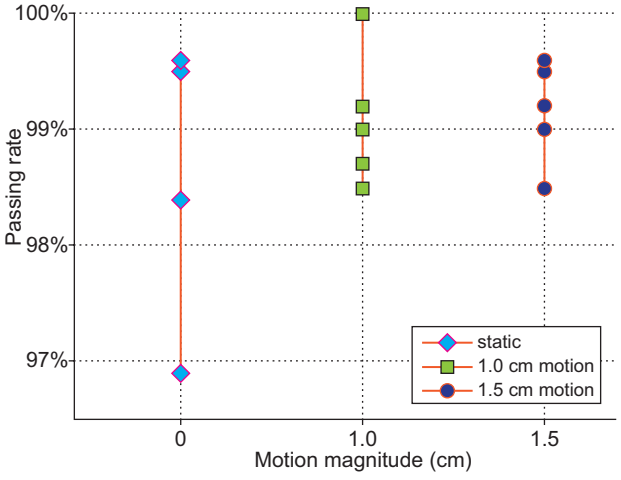

Figure 3. IMRT QA passing rates between static measurements and static VDMs (cyan diamond), and between the dynamic measurements and the motion-convolved VDMs for magnitudes of motion of 1 cm (green squares) and 1.5 cm (blue circles) for all 5 patients.

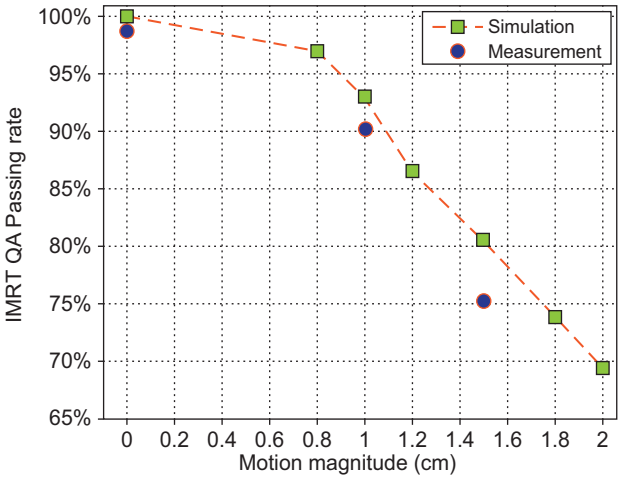

Figure 4. Correlation of the average IMRT QA passing rate of all 5 patients to the magnitude of motion. The simulated diode measurements (green squares) and the dynamic diode measurements (blue circles) were compared with the static VDMs.

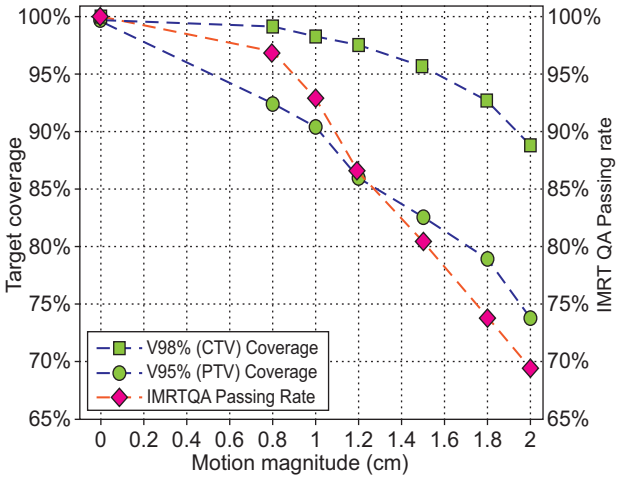

Figure 5. Correlation of the target coverage, represented by the $V_{98\%}$ of the CTV (green squares) and $V_{95\%}$ of the PTV (green circles), to the magnitude of motion. The simulated IMRT QA passing rates (magenta diamonds) were re-plotted from Figure 4 for direct comparison with the coverage.

~69% for the magnitude of 2.0 cm. On the contrary, the CTV coverage was maintained when the magnitude was <1.0 cm, but nevertheless started to decrease as the motion increased beyond 1.0 cm. The $V_{98\%}$ of the CTV was ultimately reduced by 11% when the magnitude of tumor motion was 2.0 cm.

Figure 6 shows the relationships of the magnitude of motion to the DVH of OARs. The dose to the OARs (small bowel, liver, stomach, and kidneys) was not affected significantly by tumor motion for the range of magnitudes considered, though it generally increased in the low-dose regions and decreased in the high-dose regions as the magnitude of motion increased. This ten-

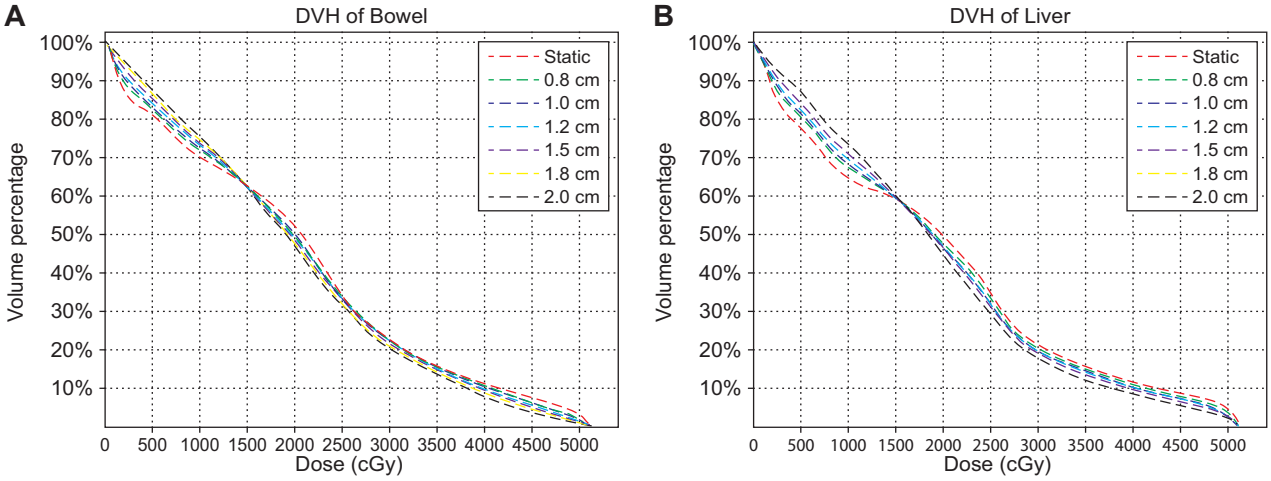

Figure 6. DVH of bowel **(A)** and liver **(B)** for different magnitudes of motion.

dency resulted from the excursions of the organs, during which the normally low-dose regions shifted into locations receiving higher doses, and *vice-versa*.

Discussion

Numerous mathematical methods have been designed to correct for the detrimental effect of organ motion during IMRT, including dose and fluence convolution methods, Monte Carlo simulations, and time-dependent computational algorithms [20,23]. In the current study, we tested and verified the effectiveness of the convolution method to calculate the dose absorbed by moving targets. In 2003 Jiang et al. performed a similar experiment for lung IMRT treatments [24], verifying the statistical model proposed in 2002 by Bortfeld et al. [11]. Their experiment had a 2D diode array placed on a platform that traced out a sinusoidal wave, in order to obtain the probability distribution of the dose to a single point. Likewise, in 2010 Waghorn et al. verified an innovative computational algorithm, which was designed to calculate the dosimetric change within patient CT data due to organ motion, by irradiating a 4D phantom using extended dose response film [25]. The study focused on step-and-shoot IMRT and solid compensator IMRT plans.

We placed a 2D diode array on a moving platform that simulated pancreatic tumor motion in order to obtain in-beam sliding-window measurements of dose maps that resulted from this motion. Concurrently, we performed a motion convolution on the PVPs to mathematically examine the effects of pancreatic tumor motion. The feasibility of the use of the convolution method to investigate the dosimetric effect of tumor motion is reflected by the good agreement between the dynamic measurements and motion-convolved VDMs derived from the convolution method (Figures 2 and 3).

The low IMRT QA passing rates for the dynamic diode measurements relative to the static verification plans (Figures 1 and 4 and Table 1) indicate that, if the static plan is not corrected for tumor motion, the dose distribution of an actual treatment delivery can deviate significantly from the distribution in the TPS (passing rate=75% for largest magnitude of motion and strictest criteria), possibly leading to erroneous dosimetric predictions. As expected, the dynamic measurements are much more similar to their motion-convolved verification plans (Figures 2 and 3), with the near-perfect passing rates between these two strongly suggesting that the motion-convolved dose distributions provide accurate calculations of the actual doses to the moving target. When evaluating a dose distribution in the TPS, therefore, it seems best to use the motion-convolved dose distribution, rather than the static dose distribution, to accurately assess the dose to the tumor under motion. These results follow the pattern of those of McCarter et al. who in 2000 mathematically tested the use of the convolution method for fractionated dose delivery [26]. Specifically, they compared the dose distributions generated in the TPS by the convolution method to those calculated by summing the doses from the fractions and modeling the random changes in target position between fractions. The results showed that even for plans with a relatively small number of fractions, the distributions calculated by the convolution method were much more accurate than those of the static plans.

The magnitudes of motion for the dynamic diode measurements were limited because the driven platform was designed to move with only a few discrete magnitudes; the two amplitudes of 1.0 cm and 1.5 cm were therefore selected for these measurements. The simulated measurements, on the contrary, could allow for

any magnitude of motion since they were derived mathematically from the convolution method. Thus, the convolution method provides the advantage of the ability to investigate the dosimetric variation for all possible amplitudes, as shown in Figure 4.

After verifying the applicability of the convolution method, we employed it for the actual patient plans in the TPS in order to analyze the dose to the moving target and the OARs. As shown in Figure 5, the CTV coverage was maintained (~100%) when the magnitude of tumor motion was <1.0 cm, indicating that pancreatic IMRT plans are relatively unaffected when the motion remains within the margin of the PTV. The CTV began to lose coverage, however, as the amplitude increased to >1.0 cm, ultimately suggesting that a predetermined margin for all pancreatic tumors should not be employed in the clinical setting. Use of such a margin for all patients may lead to a significant under-dosing of the target for those cases in which the magnitudes of motion are larger than the margin, and may result in serious toxicity to the OARs for those cases that feature smaller tumor motion. Because pancreatic motion varies greatly among patients, it is necessary to evaluate each patient's case and to use the internal treatment volume (ITV) to appropriately consider tumor motion [13]. To maintain the expected dose distributions, we can utilize mechanisms for controlling breathing or tracking motion to reduce ITV. This includes radio frequency guided radiation therapy, breath hold, respiratory gating, and active breathing control.

Relative to the CTV coverage, the $V_{95\%}$ of the PTV and the IMRT QA passing rate were affected more by the tumor motion. The poor PTV coverage was due to the lack of a safety margin for movement of the area outlined by the PTV, so that when this region shifted from its planned position, it immediately lost dose and ultimately led to the sensitive IMRT QA passing rates in the study. Analysis of the passing rates was based upon a region of interest (ROI) selected by a threshold criterion; because the ROI selected by the typical criterion of TH=10% included the whole PTV region, the passing rates were low when the diode array moved. This effect is shown in Figure 1, in which the majority of the failed points is in the peripheral regions of the ROI and is cold because of the lost coverage. The declining pattern of the IMRT QA passing rates thus followed more closely to the trend of the PTV coverage than to that of the CTV coverage; consequently, a low IMRT QA passing rate measured with the moving diode array does not always imply poor coverage of the CTV. For a magnitude of motion of 1.0 cm, for example, the IMRT QA passing rate of the dynamic diode measurements with respect to the static verification maps was ~90%, while the CTV coverage was almost 100%.

Gierga et al. [8] have studied the interplay between dynamic multileaf collimator motion and intrafractional tumor motion. They used an effective fluence algorithm, which coupled the IMRT leaf sequence files with the patient-specific target motion, to simulate the effect of tumor motion on IMRT dose distributions. Although the results showed that the application of tumor motion to their plans did not lead to a significant degradation in the target dose-volume histogram in most cases (4 of 5), the dosimetric effect of an inadequate tumor margin was not illustrated, since the range of tumor motion remained within the treatment margin used in their study. This aspect may be significant since statistical analysis has shown that the dosimetric effect of intrafractional tumor motion is subtle [11], introducing greater consequence on inappropriate margins for IMRT plans.

Figure 4 shows that the passing rates of the simulations relative to the static VDMs are always higher than the corresponding rates of the real measurements relative to the static VDMs. This result derives from the superiority, in four aspects, of the simulated measurements to the real ones. First, the dynamic MLC gap width, the positioning of dynamic MLC movement, the leaf leakage, and the tongue and groove effect cannot be simulated accurately in the TPS [27], preventing the exact calculation of the actual machine delivery by the TPS. Second, the real measurements are subject to setup errors (alignment of the diode array with the cross hairs, setup SSD with optical distance indicator) [27], while the simulated ones are not. These errors also affect measurements made in the absence of motion, and are reflected in the fact that the passing rate for static plans are less than 100% (Table 1 and Figures 3 and 4). Third, in the convolution model, the initial phase of the motion is not varied, whereas in the real measurements and in real patients, treatments start and finish at random phases of motion, ultimately resulting in differences between the measurements and the calculations of the convolution model. Finally, the interplay between the dynamic multileaf collimator and the intrafractional tumor motion in the IMRT plans was a factor in the real measurements, but was not in the convolution model. The interplay effect was reported to be a subtle effect that is made negligible by averaging multiple fractions [8,11]. In particular, Bortfeld et al. showed that the standard deviation of the distribution of dose measurements at a point, by averaging 3 measurements, reduced from 10% to 1.4% [11]. Since our results are based on the average of 3 separate measurements, the effect due to the random starting phase and interplay effects should have been reduced significantly.

In this study, we used a homogeneous phantom and the dose convolution method, which did not include heterogeneity correction. In addition, pancreatic tumor

motion is not rigid, but may involve significant deformation throughout [10]. The ability of the driven motor to only provide sinusoidal motion, therefore, limited the accuracy of our models of pancreatic motion; however, numerous studies involving tumor motion have used similar approximations [11, 21, 24-26]. Furthermore, the convolution method to the patient plans were based on the nature of organ motion, which is not limited by the sinusoidal wave.

To our knowledge this study was the first to consider the full range of amplitudes of tumor motion, which was the factor of greatest impact for the pancreatic dose distribution. The results herein reported may therefore provide guidance in the use of IMRT for the treatment of pancreatic cancer.

References

1. Ben-Josef E, Shields AF, Vaishampayan U et al. Intensity-modulated radiotherapy (IMRT) and concurrent capecitabine for pancreatic cancer. Int J Radiat Oncol Biol Phys 2004; 59: 454-459.
2. Spalding AC, Jee KW, Vineberg K et al. Potential for dose-escalation and reduction of risk in pancreatic cancer using IMRT optimization with lexicographic ordering and gEUD-based cost functions. Med Phys 2007; 34: 521-529.
3. Milano MT, Chmura SJ, Garofalo MC et al. Intensity-modulated radiotherapy in treatment of pancreatic and bile duct malignancies: Toxicity and clinical outcome. Int J Radiat Oncol Biol Phys 2004; 59: 445-453.
4. Landry JC, Yang GY, Ting JY et al. Treatment of pancreatic cancer tumors with intensity-modulated radiation therapy (IMRT) using the volume at risk approach (VARA): Employing dose-volume histogram (DVH) and normal tissue complication probability (NTCP) to evaluate small bowel toxicity. Med Dosim 2002; 27: 121-129.
5. Brown MW, Ning H, Arora B et al. A dosimetric analysis of dose escalation using two intensity-modulated radiation therapy techniques in locally advanced pancreatic carcinoma. Int J Radiat Oncol Biol Phys 2006; 65: 274-283.
6. van der Geld YG, van Triest B, Verbakel W et al. Evaluation of four-dimensional computed tomography-based intensity-modulated and respiratory-gated radiotherapy techniques for pancreatic carcinoma. Int J Radiat Oncol Biol Phys 2008; 72: 1215-1220.
7. Murphy MJ, Martin D, Whyte R et al. The effectiveness of breath-holding to stabilize lung and pancreas tumors during radiosurgery. Int J Radiat Oncol Biol Phys 2002; 53: 475-482.
8. Gierga DP, Chen GT, Kung JH et al. Quantification of respiration-induced abdominal tumor motion and its impact on IMRT dose distributions. Int J Radiat Oncol Biol Phys 2004; 58: 1584-1595.
9. Bussels B, Goethals L, Feron M et al. Respiration-induced movement of the upper abdominal organs: a pitfall for the three-dimensional conformal radiation treatment of pancreatic cancer. Radiother Oncol 2003; 68: 69-74.
10. Feng M, Balter JM, Normolle DP et al. Characterization of Pancreatic Tumor Motion Using Cine-MRI: Surrogates for Tumor Position Should be Used With Caution. Int J Radiat Oncol Biol Phys 2009; 74: 884-891.
11. Bortfeld T, Jokivarsi K, Goitein M et al. Effects of intra-fraction motion on IMRT dose delivery: Statistical analysis and simulation. Phys Med Biol 2002; 47: 2203-2220.
12. International Commission on Radiation Units and Measurements (ICRU). Report number 50: Prescribing, recording and reporting photon beam therapy. Washington DC: ICRU, 1993.
13. ICRU. Prescribing, Recording and Reporting Photon Beam Therapy (Supplement to ICRU Report 50). Report 62. Bethesda, MD: International Commission on Radiation Units and Measurements, 1999.
14. http://www.sunnuclear.com/medPhys/patientqa/mapcheck/mapcheck.asp
15. Jursinic PA, Nelms BE. A 2-D diode array analysis software for verification of intensity modulated radiation therapy delivery. Med Phys 2003; 30: 199-206.
16. Létourneau D, Gulam M, Yan D, Oldham M, Wong JW. Evaluation of a 2D diode array for IMRT quality assurance. Radiother Oncol 2004; 70: 799-805.
17. Nelms BE, Simon W. A survey on planar IMRT QA analysis. J Appl Clin Phys 2007; 8: 76-90.
18. Both S, Alecu M, Stan AR et al. A study to establish reasonable action limits for patient-specific quality assurance in intensity-modulated radiation therapy. J Appl Clin Phys 2007; 8: 1-8.
19. Lujan AE, Larsen EW, Balter JM, Ten Haken RK. A method for incorporating organ motion due to breathing into 3D dose calculations. Med Phys 1999; 26: 715-720.
20. Chetty IJ, Rosu M, Tyagi N et al. A fluence convolution method to account for respiratory motion in three-dimensional dose calculations of the liver: a Monte Carlo study. Med Phys 2003; 30: 1776-1787.
21. Trofimov A, Rietzel E, Lu HM et al. Temporo-spatial IMRT optimization: concepts, implementation and initial results. Phys Med Biol 2005; 50: 2779-2798.
22. MATLAB version 7.9.0 Natick, Massachusetts: The MathWorks Inc., 2009.
23. Chui CS, Yorke E, Hong L. The effects of intra-fraction organ motion on the delivery of intensity-modulated field with a multileaf collimator. Med Phys 2003; 30 1736-1746.
24. Jiang SB, Pope C, Al Jarrah KM, Kung JH, Bortfeld T, Chen GT. An experimental investigation on intra-fractional organ motion effects in lung IMRT treatments. Phys Med Biol 2003; 48: 1773-1784.
25. Waghorn B, Shah AP, Ngw AW et al. A computational method for estimating the dosimetric effect of intra-fraction motion on step-and-shoot IMRT and compensator plans. Phys Med Biol 2010; 55: 4187-4202.
26. McCarter SD, Beckham WA. Evaluation of the validity of a convolution method for incorporating tumour movement and setup variations into the radiotherapy planning system. Phys Med Biol 2000; 45: 923-931.
27. Ezzell GA, Burmeister JW, Dogan N et al. IMRT commissioning: Multiple institution planning and dosimetry comparisons: a report from AAPM Task Group 119. Med Phys 2009; 36: 5359-5373.